

This is the post-print version of the following article: Llop, J; Lammers, T. [Nanoparticles for Cancer Diagnosis, Radionuclide Therapy and Theranostics](#), ACS Nano 2021, 15, 11, 16974–16981

DOI: [10.1021/acsnano.1c09139](https://doi.org/10.1021/acsnano.1c09139)

This article may be used for non-commercial purposes in accordance with ACS Terms and Conditions for Self-Archiving.

# Nanoparticles for Cancer Diagnosis, Radionuclide Therapy and Theranostics

*Jordi Llop<sup>1,\*</sup>, Twan Lammers<sup>2,†</sup>*

<sup>1</sup> Radiochemistry and Nuclear Imaging Group, CIC biomaGUNE, Basque Research and Technology Alliance (BRTA), 20014 San Sebastian, Spain.

<sup>2</sup> Department of Nanomedicine and Theranostics, Institute for Experimental Molecular Imaging (ExMI), RWTH Aachen University Clinic and Helmholtz Institute for Biomedical Engineering, 52074 Aachen, Germany.

## KEYWORDS

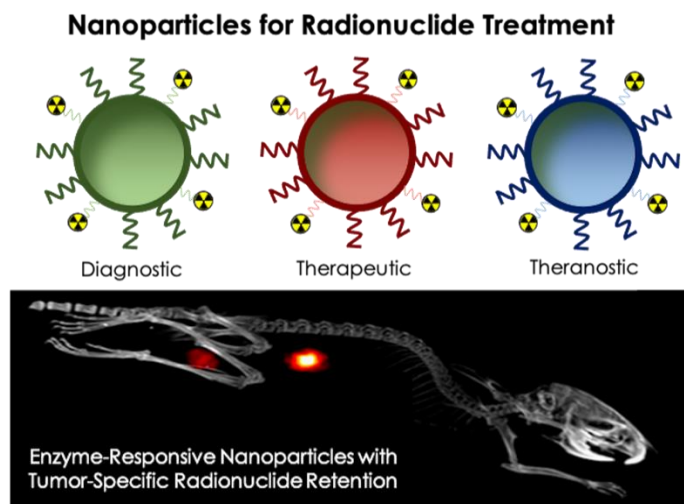
Nanoparticles, diagnostics, theranostics, imaging, radiopharmaceutical therapy.

## ABSTRACT

Nanoparticles have unique properties which can be exploited for cancer diagnosis and therapy. Intravenously injected nanoparticles accumulate, besides in tumors and at sites of inflammation and infection, predominantly in organs of the mononuclear phagocytic system. Accumulation in liver and spleen lowers nanoparticles' ability to target pathological sites, and it compromises their use for radionuclide therapy. Recent work shows that radionuclide retention in liver and spleen can be greatly reduced by using liposomes surface-modified with esterase-cleavable radionuclide

anchors. Since esterase activity is high in healthy tissues and low in tumors, liposome-associated radioactivity rapidly cleared from the body and remained high only in tumors, producing impressive images, with high contrast-to-background ratios and remarkable tumor delineation. We here put these advances in perspective from an early detection, cancer diagnosis, radionuclide therapy and theranostics point of view. We briefly outline the current clinical landscape of radionuclide targeting, imaging and therapy, and reflect on the role(s) that nanoparticles can play in these applications. We highlight the potential of nanoparticles responsive to endogenous stimuli for intra-operative imaging and particularly for individualized and improved radionuclide treatment. Future studies exploring the robustness and the clinical feasibility of such nanoradiotheranostic probes and protocols are eagerly awaited.

#### GRAPHICAL ABSTRACT



## MAIN TEXT

### **1. Introduction:**

Nanoparticles (NP) are extensively used for biomedical applications. They have multiple unique physicochemical features, including a large surface-to-volume ratio, an arsenal of surface functionalization possibilities, and the capacity to carry large amounts of cargo. These properties, together with the vast variety of materials that can be utilized for their preparation, open up an almost unlimited number of opportunities in biomedicine and beyond.

NP can be engineered to be biocompatible and stable in biological fluids, and they can be endowed with various imaging capabilities, via incorporating fluorescent agents, radionuclides and (super-) paramagnetic materials. NP take advantage of pathophysiological features, most notably the enhanced permeability and retention (EPR) effect, to localize in target sites. In the case of cancer, EPR enables passive accumulation in tumors upon intravenous administration as a result of fenestrations in leaky blood vessels coupled to impaired lymphatic drainage.<sup>1-2</sup> This preferential accumulation at pathological sites – which besides on classical EPR features has recently been shown to also rely on active transcytosis across vascular endothelium<sup>3</sup> and on retention in tumor-associated macrophages (TAM) acting as a reservoir<sup>4</sup> – has been widely exploited in the past couple of decades for the development of diagnostic, therapeutic and theranostic nanomaterials.

Besides in tumors, NP with sizes above 5-10 nm typically show high levels of accumulation in organs of the mononuclear phagocytic system (MPS; formerly known as reticuloendothelial system (RES)), particularly in liver and spleen. These organs possess features similar to those driving EPR and tumor accumulation, *i.e.* high blood vessel density, fenestrated vasculature and prominent presence of phagocytes. NP accumulation in MPS organs results in a decrease in the particles' availability in the blood stream and it lowers their chances of efficiently accumulating

at pathological sites. Some have argued that prominent accumulation of NP in liver and spleen might result in side effects in these organs, but clinically not much evidence is available to back up these concerns.

Over the years, many efforts have been undertaken to lower MPS uptake (kinetics), in order to eventually improve NP target site accumulation. These have encompassed pharmacological approaches, *e.g.*, reducing the number of liver Kupffer cells via pre-treatment with liposomal clodronate,<sup>5</sup> as well as materials-focused strategies, based on changing key NP properties such as size,<sup>6-8</sup> shape<sup>9</sup> and surface composition.<sup>10</sup> Thus far, the added value and clinical impact of these approaches have remained modest, apart from the pioneering discovery more than 30 years ago that liposome surface modification with poly(ethylene glycol) (PEG) prolongs circulation times and improves tumor accumulation and antitumor efficacy.<sup>11-13</sup>

## **2. Diagnostics Nanoparticles Evading the MPS**

Writing in the a recent issue of ACS Nano, Lee and coworkers present an elegant approach to achieve very high liposomal tracer uptake in tumors, while preventing signal retention in liver and spleen.<sup>14</sup> In their paper entitled “Imaging Strategy that Achieves Ultrahigh Contrast by Utilizing Differential Esterase Activity in Organs: Application in Early Detection of Pancreatic Cancer”, they describe PEG-liposomes incorporating iodine-124 (<sup>124</sup>I) and iodine-131 (<sup>131</sup>I). The former is a diagnostic radionuclide with a relatively long physical half-life of 4.18 days, enabling non-invasive visualization and quantification of NP biodistribution and tumor accumulation *in vivo* via positron-emission tomography (PET). The latter is the most used iodine radioisotope, and is typically utilized for therapeutic and theranostic applications.

The originality of Lee *et al.*'s approach lies in the method of radiolabel-anchoring. In their liposomes, the radiolabel is linked to one of the membrane components through esterase-labile

ester bonds (Fig. 1A). As controls, they employed liposomes radiolabeled via non-cleavable linkers. The reasoning behind this approach is that esterase activity is high in healthy tissues and deregulated (absent) in tumors. After intravenous administration in mice bearing CT26 murine colorectal carcinoma tumors, uptake in tumor, liver, and spleen, as well as tracer elimination via the urine was observed for all formulations. Strikingly, however, as opposed to control liposomes (Fig. 1B), the PET signals associated with liposomes with esterase-labile linkers completely cleared from liver and spleen within 24 hours after administration (Fig. 1C). Apart from some residual activity in bladder and thyroid (resulting from not completely stable iodine labeling), the only signals observed were in tumors, generating stunning images, with impressive signal-to-background ratio and very good tumor delineation (Fig. 1C).

Via a battery of *in vitro* and *ex vivo* experiments, Lee *et al.* demonstrated that the clearance from MPS organs depended on the presence of esterases, which induced selective chemical bond cleavage of the radioactive anchor, resulting in the formation of 4-iodobenzoic acid and rapid elimination from the body. The authors went on to show that surface decoration of the esterase-labile  $^{124}\text{I}$ -liposomes with folate as a targeting ligand boosted the tumor signal-to-background ratio. Accordingly, active ligand targeting achieved relatively selective signal generation in folate receptor-positive PANC-1 versus folate receptor-negative MIA PaCa-1 pancreatic xenograft tumors. The authors furthermore verified the tracer potential of their esterase-labile liposomes via experiments in mice with orthotopically inoculated PANC-1 tumors, confirming that also in case of localization within the pancreas, the enzyme-responsive nanodiagnostics are able to generate impressive images with very high signal-to-background ratios (Fig. 1D).

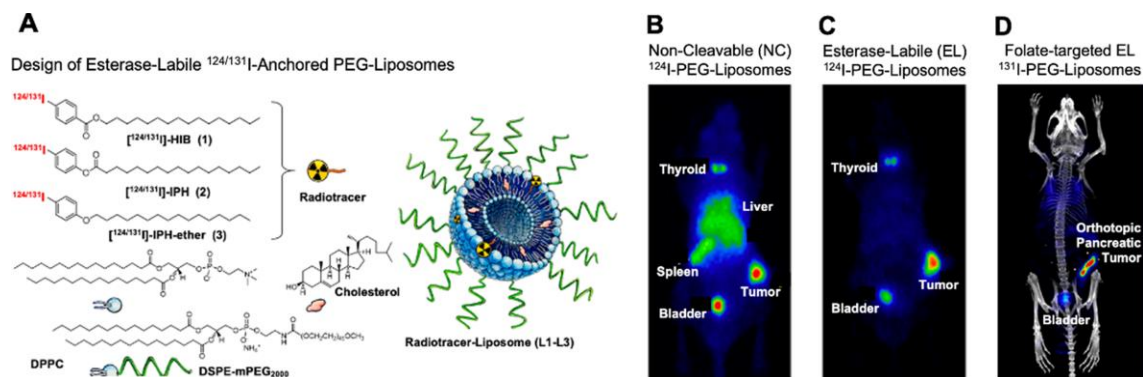


**Figure 1: Probes and protocols for tumor-targeted radionuclide therapy.** A: Design of liposome-based radiotracers enabling MPS clearance of radioactivity via enzymatic cleavage of ester groups. Ether groups served as non-cleavable controls. B-D: PET scans of non-cleavable (B), esterase-labile (C), and folate-targeted esterase-labile liposomes (D) labeled with  $^{124}\text{I}$  and  $^{131}\text{I}$  in subcutaneous and orthotopic pancreatic tumors in mice. Images reproduced with permission from ref <sup>14</sup>.

### 3. Nanoparticles for Cancer Diagnosis

Based on the results reported, Lee and colleagues enthusiastically propose “a potential widely applicable foundation for the rational design and development of various imaging agents for sensitive early tumor detection with ultrahigh contrast”. While undeniably being a major step forward towards the *in vivo* application of NP for sensitive and specific tumor detection, some reservations appear to be appropriate here.

These include: (1) a realistic reflection on early cancer detection and the role of radionuclide imaging therein; (2) the dependence of liposome tumor accumulation on EPR, which is highly variable and thus may lead to many false negatives; and (3) the modest added value of avoiding the MPS when using nanoparticles as contrast agents to detect tumors. Building upon the results presented, another key question to ask is: (4) in which clinically meaningful scenarios would

esterase-responsive radionuclide-shedding liposomes actually add value from a diagnostic, therapeutic and/or theranostic point-of-view?

### **3.1. Non-invasive Imaging vs. Early Cancer Detection**

Functional and molecular imaging techniques, and particularly PET, single photon emission computed tomography (SPECT) and magnetic resonance imaging (MRI), rely on the use of sophisticated equipment, which is not widely available, and which results in low throughput. In an optimistic estimation, only 10-20 patients can realistically be imaged per scanner per day. PET and to a lower extent also SPECT furthermore require well-established production and distribution networks to supply radiopharmaceuticals to imaging sites, which comes with logistic and economic burdens, largely caused by the short half-life of the radionuclides commonly used in clinical practice. Thus, as compared to low-energy X-ray imaging, which is indeed used as a screening tool for early breast cancer detection, PET and SPECT imaging are unlikely to be suitable screening tools for early cancer detection, particularly in asymptomatic individuals. This notion is corroborated by the fact that PET and SPECT are also never used as first-look diagnostic options, as opposed to several other imaging modalities, such as X-ray and ultrasound.

The use of PET or SPECT as a screening and/or early detection tool is further complicated when unconventional tracers and non-standard labeling protocols are to be used, as would be the case for NP diagnostics. NP labeling methods which – like in the study by Lee et al. – are not based on radionuclide attachment to or entrapment in preformed NP are inconvenient, as they require several synthetic and purification steps, which all involve ionizing radioactive species and which oftentimes result in relatively low radiochemical yields. Even when employing post-loading methods to label NP, strict regulations mandate good manufacturing practice (GMP)-compliant production processes, as well as exhaustive quality-control (QC) procedures to assess the

morphological, structural, chemical and radioactive properties of the radiopharmaceutical.<sup>15</sup> Equipment for NP characterization is typically located outside of radiation-protection areas, hampering the broad-scale GMP-based production and QC characterization that are needed before agents can be administered to patients. Together, these insights and aspects compromise the usefulness of radiolabeled NP as tools for cancer screening and early tumor detection.

### **3.2. Diagnostic Accuracy vs. EPR-based Nanoparticle Accumulation in Tumors**

A key aspect of (early) cancer detection is diagnostic accuracy. Diagnostic accuracy refers to the ability of a liquid, biopsy, or imaging biomarker to both sensitively and specifically discriminate between a case condition in which a disease is present (true positive), and a condition in which the disease is absent (true negative). Moreover, and arguably even more importantly, conditions should be avoided in which the biomarker provides false positive or false negative information. In such situations, healthy individuals are informed that they have cancer, and cancer patients are informed that they are healthy. Both situations have deleterious consequences.

An important drawback of enzyme-responsive liposomal radiotracers – and of nanodiagnostics for tumor detection in general – is that EPR-mediated NP tumor accumulation is highly heterogeneous.<sup>16-17</sup> This results from very high inter- and intra-individual variability in the pathophysiological features driving NP tumor accumulation, such as vascular density, perfusion and permeability, endothelial transcytosis, tumor stroma density and penetrability, lymphatic functionality, and TAM presence and polarization.<sup>18</sup> While the results presented by Lee and colleagues are overall promising, one needs to take into account that with such probes and protocols, there may be a number of cancerous lesions that go unnoticed, because they do not present with sufficiently high levels of EPR and tumor accumulation. Diagnostically, these lesions would be false negatives, and clinically, they would be misdiagnosed as non-cancerous.

### 3.3. Tumor Detection vs. Suppressing MPS Signal

Contrast is crucial for *in vivo* imaging. Rather than just achieving a high uptake of a contrast agent at the pathological site, the difference in uptake between pathological tissue and surrounding healthy tissue is key for accurate diagnosis and staging. Consequently, the esterase-responsive NP developed by Lee *et al.* arguably only add value in case of tumor detection of liver and spleen. For detecting tumors in other organs, non-cleavable liposomes would probably do an equally good job as esterase-responsive liposomes, as MPS uptake and retention in such situations does not compromise tumor detection.

A noteworthy example to compare to here is the use of superparamagnetic iron oxide NP (SPION) as MRI contrast agents for the detection of liver tumors. After i.v. administration, SPION are sequestered by Kupffer cells in the liver, thus producing strong T2/T2\* relaxation effects in normal hepatic parenchyma and not in cancer lesions (where the NP accumulate significantly less efficiently), generating good contrast between tumors and surrounding healthy tissue.<sup>19</sup> This indicates that the approach can in principle work for detecting liver lesions. It needs to be taken into account, however, that well-established, well-functioning and perfectly biocompatible alternatives are available for contrast-enhanced detection of liver tumors, including the use of the small-molecule MRI contrast agent gadolinium-ethoxybenzyl-dimeglumine (Gd-EOB-DTPA; marketed as Primovist® in Europe and as Eovist in the USA®). This raises the question whether there is really a need for developing new contrast agents and imaging approaches for liver cancer detection.

A potentially interesting approach that relates to the above reasoning is the use of enzyme-responsive liposomes not labeled with radioisotopes, but with fluorophores or with photoacoustic contrast agents. Targeted imaging tracers, based on small molecules (e.g. folate), peptides,

antibodies and also nanoparticles, are increasingly explored for tumor identification and margin detection in surgical theatres.<sup>20-21</sup> Promising proof-of-concept for the use of responsive NP for fluorescence-guided surgery has recently been provided, including in patients, showing that pH-activatable ONM-100 micelles loaded with indocyanine green (ICG) were able to detect tumor-positive resection margins in 9 out of 9 subjects, and furthermore identified 4 otherwise missed occult cancer lesions.<sup>22</sup> Similar directions and applications are also conceivable for the enzyme-responsive liposomal platform developed by Lee *et al.*

#### **4. Radionuclide Therapeutics and Theranostics**

Beyond exploring the enzyme-responsive liposomes developed by Lee *et al.* for cancer diagnosis, we here argue that this smartly designed NP platform may also find application as a theranostic agent, particularly in the context of radiopharmaceutical therapy (RPT). RPT is based on the targeted delivery of radioactive atoms, mainly  $\beta$ -emitting particles or highly potent  $\alpha$ -emitting particles.<sup>23</sup> In RPT, both the total dose and the rate at which the dose is delivered to tumors vs. normal tissues define treatment success. Hence two key questions in RPT are: (1) Where does the radioactivity localize? And (2) for how long does the radioactivity remain at the target site vs. at off-target sites? To assist in answering these questions, initial pre-therapy imaging is performed with diagnostic positron- or gamma-emitters, instead of with therapeutic  $\alpha$ - or  $\beta$ -emitters. This is done to obtain non-invasive and quantitative imaging information on on-target vs. off-target accumulation without already having to expose patients to potentially harmful radionuclides. This theranostic setup aids in patient stratification, dose selection and prediction of therapeutic outcome. In this context, high concentrations and long residence times within tumors, coupled to low accumulation and fast clearance from healthy tissues, constitute the ideal RPT scenario.

##### **4.1. Iodine**

A prototypic example of RPT is radioiodine treatment. I.v. administered iodine is concentrated in thyroid follicular cells and differentiated follicular thyroid cancer cells via the sodium–iodide symporter, and it does not accumulate anywhere else. Iodine-based RPT thus presents an attractive treatment option for the management of thyroid malignancies.<sup>24</sup> As a consequence, RPT using the  $\beta$ -emitter  $^{131}\text{I}$  remains the recommended treatment for patients with metastatic differentiated thyroid cancer. In such setups, diagnostic pre- and post-treatment scans are conducted with the gamma-emitting isotope  $^{123}\text{I}$ . Radioiodine therapy is very straightforward, and it has cure rates exceeding 90%, which is great, but there is one major limitation: it only works in one cancer type.

#### **4.2. Somatostatin Receptor-targeted Probes**

Expansion of RPT for use in non-thyroid tumors has necessitated the development of somewhat more complex radiopharmaceuticals. These typically consist of radionuclides connected to “targeting vehicles” capable of concentrating at pathological sites via receptor-ligand interactions. Peptide-based targeting vehicles directed towards the somatostatin receptor (SSTR), such as DOTATOC and DOTATATE, have represented a major breakthrough in the clinical implementation of RPT. Both DOTATOC and DOTATATE labeled either with  $^{177}\text{Lu}$  or  $^{90}\text{Y}$  are currently used for the treatment of SSTR-positive neuroendocrine tumors (NET), pheochromocytomas and paragangliomas.<sup>25</sup> For companion diagnostics, pre- and post-treatment PET scans with  $^{68}\text{Ga}$ -labeled DOTATOC or DOTATATE are carried out. This is done for multiple reasons, including identification of the presence of SSTR-positive lesions capable of accumulating the radiopharmaceutical and hence potentially responding to RPT treatment (Fig. 2A, left), as well as evaluation of treatment efficacy and guidance of clinical decision-making regarding follow-up interventions (Fig. 2A, right).<sup>26</sup> Importantly, the companion diagnostic PET images also reveal significant kidney accumulation, indicating potential toxicity of RPT towards the kidneys. The

kidney accumulation of peptide-based RPT agents can be suppressed via the coadministration of basic amino acids (lysine, arginine), bovine gelatin-containing solutions or albumin fragments <sup>27</sup>. As these blocking agents are not working optimally, the accumulation and retention of peptide-based RPT agents in the kidney result in side effects potentially leading to loss of renal function, as well as to reductions in the RPT dose that can be repeatedly administered to patients, thus limiting the chances for good therapeutic responses.

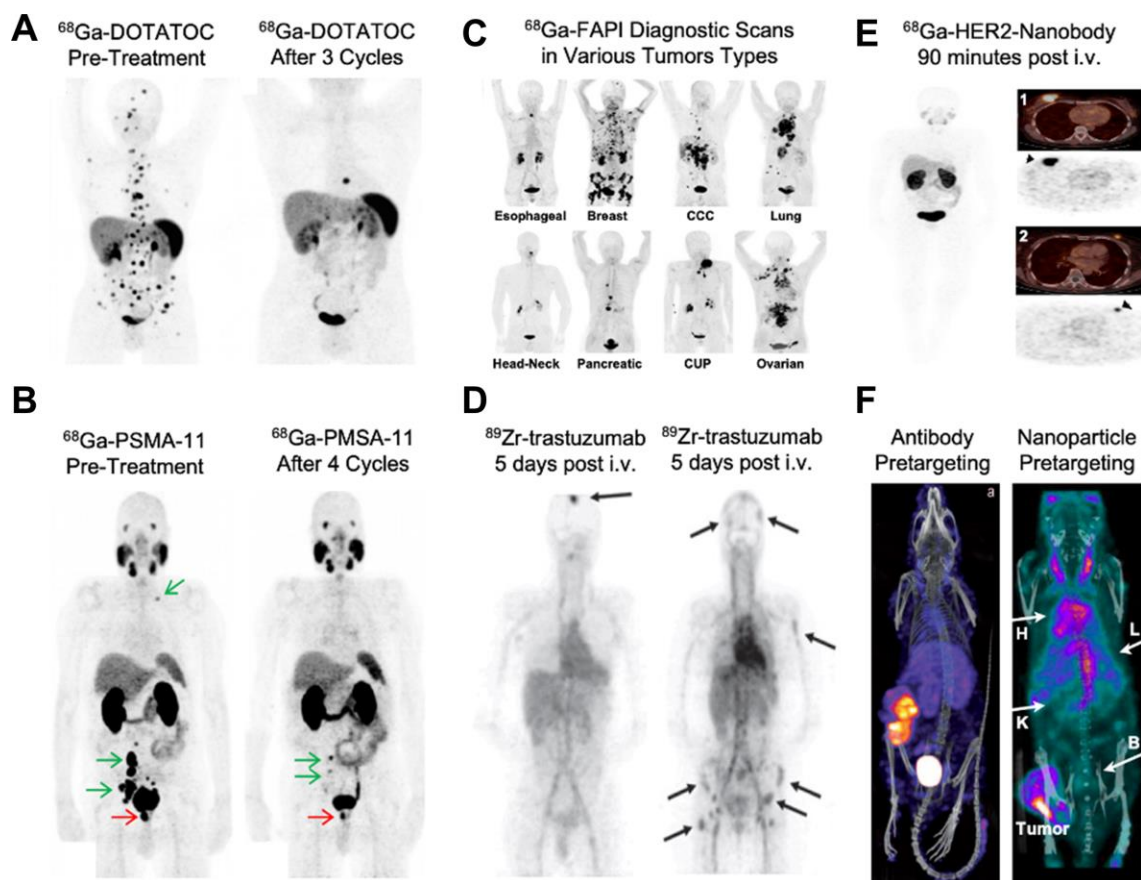


**Figure 2. Tumor-targeted radionuclide therapy.** A: PET scans of somatostatin receptor-targeted <sup>68</sup>Ga-DOTATOC in a patient with atypical lung carcinoids before and after peptide receptor-based radionuclide therapy (2 cycles <sup>90</sup>Y-DOTATOC and 1 cycle <sup>177</sup>Lu-DOTATATE). B: PET scans obtained using <sup>68</sup>Ga-PSMA-11 in a patient with metastatic castration-resistant prostate cancer prior

to and after 4 cycles of radiopharmaceutical therapy with  $^{177}\text{Lu}$ -PSMA-617. C: PET scans obtained using cancer-associated fibroblast-targeted  $^{68}\text{Ga}$ -FAPI exemplify probe enrichment in various different tumor types. D: Biodistribution and target site localization of the  $^{89}\text{Zr}$ -labeled and HER2-specific antibody trastuzumab at 5 days after i.v. administration in breast cancer patients with brain and bone metastases. E: Biodistribution and tumor accumulation of HER2-specific nanobodies labeled with  $^{68}\text{Ga}$  at 90 minutes after i.v. injection in patients with high (1) and medium (2) HER2 expression in breast tumors. F: Pretargeting approaches based on the initial injection of *trans*-cyclooctyne-modified antibodies (anti-TAG72; left) or nanoparticles (Peptobrushes; right), followed by a waiting time and then injection of tetrazine-based chelators labeled with  $^{111}\text{In}$ . Images reproduced with permission from refs <sup>26, 28-33</sup>

### **4.3. PSMA- and FAP-targeted Probes**

Two other RPT examples that have been making headlines in recent years are probes targeted to the prostate-specific membrane antigen (i.e., PSMA; a transmembrane protein highly overexpressed in prostate cancer) and the fibroblast activation protein (i.e, FAP; a membrane-anchored protease overexpressed by cancer-associated fibroblasts). For PSMA, clinical trials have convincingly demonstrated the theranostic potential of RPT ligand pairs to treat metastatic castration-resistant prostate cancer.<sup>34-35</sup> Pre-treatment PET scans with diagnostic  $^{68}\text{Ga}$ -labeled PSMA probes aid in the identification of primary and metastatic prostate cancer lesions (Fig 2B), and they help to individualize and improve  $^{177}\text{Lu}$ -PSMA-probe therapeutic outcomes (Fig. 2B).<sup>28</sup> Analogously, FAP-targeted agents have been explored, initially as diagnostic tools and nowadays increasingly also as therapeutic (theranostic) agents.  $^{68}\text{Ga}$ -labeled FAP-targeted probes, such as FAPI-02 and FAPI-04, provide impressive PET images, with very high tumor-to-background ratios in patients with a wide range of cancers, suggesting high potential for FAP-targeted

diagnostics and theranostics.<sup>29</sup> However, both PSMA- and FAP-targeted probes do have several important downsides. These include off-target accumulation in the kidney, similar to DOTATOC and DOTATE, potentially causing kidney damage. PSMA-targeted probes furthermore show high uptake in submandibular and parotid glands, as well as in gastrointestinal tract, which also results in off-target toxicity (Fig. 2B). Another important issue, particularly obvious for currently used FAP-targeted agents, is (too) short on-target retention, which has limited the therapeutic and theranostic potential of FAP-based RPT.<sup>36-37</sup>

#### **4.4. Antibodies**

To overcome the above limitations, multiple other probes and protocols are being explored for RPT, including antibodies (Ab). Ab are nature's own targeting moieties, gradually optimized by evolution to efficiently engage with targets; they show high affinity and specificity, and have very long circulation times, with half-lives in the order of days to weeks. This high availability in the bloodstream promotes progressive accumulation at the target site. For imaging and RPT purposes, however, this is quite disadvantageous, as slow clearance compromises contrast at early time points after administration and as it increases systemic exposure. Consequently, Ab-based imaging is typically done with long-lived radioisotopes, multiple days after i.v. injection, and even then there is still significant background coming from signal from the blood (Fig. 2D). Additionally, Ab accumulation in solid tumors is hampered – at least to some extent – by limited diffusion capacity (as compared to smaller molecules) and by reduced penetration as a result of the so-called binding-site barrier.<sup>38-39</sup> Together, these issues explain why the clinical use of Ab-based RPT for the treatment of solid (non-hematological) tumors is very limited.

#### **4.5. Nanobodies**

The pharmacokinetic properties and systemic exposure of Ab and their fragments are primarily driven by their molecular weight. Hence, a straightforward option to shorten circulation time (and at the same time enhance diffusion capability within tumors) is to produce smaller-sized alternatives, such as nanobodies (Nb). Nb consist of an  $V_{HH}$  fragment, i.e., the smallest fragment of an antibody with antigen-binding capacity. They present with high stability, specificity, and affinity for the target antigen, as well as improved tissue penetration. Importantly, they show relatively rapid clearance from the blood, in the order of minutes to 1-2 hours, and low accumulation in healthy tissues.<sup>40</sup> As a result of this, Nb are perfectly suited for providing high-contrast images with excellent tumor delineation at short periods of time after i.v. administration (Fig. 2E).<sup>31</sup> However, like other small antibody fragments, they show relatively short tumor retention, due to their monovalent binding.<sup>41</sup> This, together with high kidney accumulation compromises their clinical use and theranostic potential.

#### **4.6. Antibody Pretargeting**

An alternative strategy to reduce the high systemic exposure of Ab-based RPT is pretargeting. This elegant concept is based on chemically and kinetically uncoupling the targeting vehicle and the radionuclide, and then rely on *in vivo* recombination chemistry to connect the two agents. In a classical pretargeting setup, the targeting vehicle – typically an Ab – is administered first, and after several days, i.e., after accumulation at the target site and clearance from blood and healthy tissues, a radiolabeled small molecule capable of selectively binding to the targeting vehicle is injected. The radiolabeled small molecule distributes all over the body and rapidly clears via the kidney, with no retention in any tissue except from those sites where the targeting vehicle is present, i.e., the tumor. Different pretargeting constructs and chemistries have been evaluated over the years. These most prominent include the interaction between streptavidin and biotin, the use of bispecific

antibodies with a binding site for a radiolabeled hapten, the sequence-specific hybridization of oligonucleotides, and biorthogonal reactions involving trans-cyclooctene (TCO) and tetrazine. The capability of pretargeting to achieve high tumor uptake and high tumor-to-blood ratios has been demonstrated preclinically in a number of studies (Fig. 2F).<sup>32, 42</sup> Despite significant promise, pretargeting approaches have not yet been implemented in routine clinical practice, for a number of reasons, including the need for administering two different components (which is a translational, regulatory and practical burden), and the difficulty of optimizing and individualizing the time gap between the two administrations.

#### **4.7. Nanoparticle Pretargeting**

Very recently, biodegradable polymeric NP have been explored as alternatives for antibody-based targeting vectors in pretargeting setups.<sup>33</sup> Contrary to antibodies, these so-called PeptoBrushes can be equipped with a very high degree of functionalization, with TCO moieties arranged into patches attracting hydrophobic tetrazine moieties. This increases biorthogonal reaction rates and thereby efficiency of in vivo click chemistry. A key feature of pretargeting in general is that the reaction between TCO and tetrazine to capture the small molecule radiolabel only occurs if the targeting vehicles are not internalized by cells. This means that NP captured by Kupffer cells in the liver and red pulp macrophages in the spleen do not undergo the click reaction; hence, the radionuclide does not accumulate and generate contrast in these organs (Fig 2F). In terms of application and outcome, this approach is very similar to the work Lee and colleagues,<sup>9</sup> generating strong signals in tumors and high contrast-to-background images, while preventing radioactivity retention in the MPS organs liver and spleen.

#### **5. Towards Next-Generation Radiotheranostics**

Textbooks state that ideal radiopharmaceuticals should be stable after administration. Lee and coworkers provide experimental evidence disproving this dogma. They show that site-selective degradation of radiopharmaceuticals favors image contrast and reduces systemic exposure to radionuclides. These features classify their liposomal NP as “intelligent” contrast agents,<sup>28</sup> capable of providing images with exquisite tumor delineation and high signal-to-noise ratios.

Beyond early diagnosis, which is monopolized by fast, cheap, high-throughput and widely available methods which need to have very high diagnostic accuracy, Lee et al.’s liposomes may open up new avenues for radionuclide therapy and theranostics. They are capable to overcome multiple of the main limitations of currently available RPT agents, i.e., fast tumor washout for small molecules, high kidney retention for peptides and nanobodies, high systemic exposure for antibodies, and practical difficulties for pre-targeting strategies, as well as the high accumulation in MPS organs that is typical for conventional non-enzyme-responsive NP.

The material developed has two additional advantages: (1) it allows for identical compounds to be used for <sup>123</sup>I/<sup>124</sup>I-based diagnostic SPECT/PET imaging and for <sup>131</sup>I-based radionuclide therapy. The availability of such identical diagnostic/therapeutic pairs enables accurate monitoring of biodistribution, precise prediction of target site accumulation and faithful imaging-based identification of responsive tumor lesions. Moreover, (2) the possibility to use both <sup>123</sup>I for SPECT and <sup>124</sup>I for PET favor clinical implementation, as hospitals can then flexibly adapt the diagnostic tracer to the imaging equipment they have available.

Before the promise of the approach can be realized in the clinic, several important questions need to be answered: Will clearance from MPS organs be as effective in humans as in mice? Will tumor retention and contrast-to-background ratios be as good in humans as in mice? How many human tumors present deregulated esterase activity? How homogenous is esterase activity in

different healthy organs and (multimorbid) patients? Additional interesting questions are: Can the technology be expanded to other theranostic radionuclide pairs? Can the technology be used for tumor delineation in image-guided surgery settings? And can the presence of other endogenous enzymes be exploited for similar purposes? Answering these questions and moving the technology forward will obviously take several additional years. If some of these questions can be answered positively, we expect to see this (and similar) technology in the clinic within the next 5 to 10 years.

## AUTHOR INFORMATION

### **Corresponding Authors**

\* Email: [jllop@cicbiomagune.es](mailto:jllop@cicbiomagune.es)

† Email: [tammers@ukkaachen.de](mailto:tammers@ukkaachen.de)

### **Author Contributions**

The manuscript was written through contributions of all authors. All authors have given approval to the final version of the manuscript.

### **Notes**

The authors declare no competing financial interest.

## ACKNOWLEDGMENT

Twan Lammers gratefully acknowledges support by the European Research Council (ERC: Meta-Targeting (CoG 864121), and the German Research Foundation (DFG: GRK 2375 (Tumor-targeted Drug Delivery; project number: 331065168), SFB 1066 and LA2937/4-1). Jordi Llop

gratefully acknowledges support by the Spanish Research Agency (Grant number PID2020-117656RB-100).

## REFERENCES

1. Matsumura, Y.; Maeda, H. A New Concept for Macromolecular Therapeutics in Cancer Chemotherapy: Mechanism of Tumoritropic Accumulation of Proteins and the Antitumor Agent Smancs. *Cancer Res* **1986**, *46* (12 Part 1), 6387-6392.
2. Maeda, H.; Sawa, T.; Konno, T. Mechanism of tumor-targeted delivery of macromolecular drugs, including the EPR effect in solid tumor and clinical overview of the prototype polymeric drug SMANCS. *J Control Release* **2001**, *74* (1-3), 47-61.
3. Sindhwani, S.; Syed, A. M.; Ngai, J.; Kingston, B. R.; Maiorino, L.; Rothschild, J.; MacMillan, P.; Zhang, Y.; Rajesh, N. U.; Hoang, T.; Wu, J. L. Y.; Wilhelm, S.; Zilman, A.; Gadde, S.; Sulaiman, A.; Ouyang, B.; Lin, Z.; Wang, L.; Egeblad, M.; Chan, W. C. W. The entry of nanoparticles into solid tumours. *Nature Materials* **2020**, *19* (5), 566-575.
4. Miller, M. A.; Zheng, Y.-R.; Gadde, S.; Pfirschke, C.; Zope, H.; Engblom, C.; Kohler, R. H.; Iwamoto, Y.; Yang, K. S.; Askevold, B.; Kolishetti, N.; Pittet, M.; Lippard, S. J.; Farokhzad, O. C.; Weissleder, R. Tumour-associated macrophages act as a slow-release reservoir of nano-therapeutic Pt(IV) pro-drug. *Nature Communications* **2015**, *6* (1), 8692.
5. Tavares, A. J.; Poon, W.; Zhang, Y.-N.; Dai, Q.; Besla, R.; Ding, D.; Ouyang, B.; Li, A.; Chen, J.; Zheng, G.; Robbins, C.; Chan, W. C. W. Effect of removing Kupffer cells on nanoparticle tumor delivery. *Proceedings of the National Academy of Sciences* **2017**, *114* (51), E10871.

6. Feng, J.; Iyer, A.; Seo, Y.; Broaddus, C.; Liu, B.; VanBrocklin, H.; He, J. Effects of size and targeting ligand on biodistribution of liposome nanoparticles in tumor mice. *Journal of Nuclear Medicine* **2013**, *54* (supplement 2), 1339.
7. Hoshyar, N.; Gray, S.; Han, H.; Bao, G. The effect of nanoparticle size on in vivo pharmacokinetics and cellular interaction. *Nanomedicine (London, England)* **2016**, *11* (6), 673-692.
8. Litzinger, D. C.; Buiting, A. M. J.; van Rooijen, N.; Huang, L. Effect of liposome size on the circulation time and intraorgan distribution of amphipathic poly(ethylene glycol)-containing liposomes. *BBA - Biomembranes* **1994**, *1190* (1), 99-107.
9. Liu, Y.; Wang, Z.; Zhu, G.; Jacobson, O.; Fu, X.; Bai, R.; Lin, X.; Lu, N.; Yang, X.; Fan, W.; Song, J.; Yu, G.; Zhang, F.; Kalish, H.; Niu, G.; Nie, Z.; Chen, X. Suppressing Nanoparticle-Mononuclear Phagocyte System Interactions of Two-Dimensional Gold Nanorings for Improved Tumor Accumulation and Photothermal Ablation of Tumors. *ACS Nano* **2017**, *11* (10), 10539-10548.
10. Suk, J. S.; Xu, Q.; Kim, N.; Hanes, J.; Ensign, L. M. PEGylation as a strategy for improving nanoparticle-based drug and gene delivery. *Advanced drug delivery reviews* **2016**, *99* (Pt A), 28-51.
11. Klibanov, A. L.; Maruyama, K.; Torchilin, V. P.; Huang, L. Amphipathic polyethyleneglycols effectively prolong the circulation time of liposomes. *FEBS Lett* **1990**, *268* (1), 235-7.

12. Papahadjopoulos, D.; Allen, T. M.; Gabizon, A.; Mayhew, E.; Matthay, K.; Huang, S. K.; Lee, K. D.; Woodle, M. C.; Lasic, D. D.; Redemann, C. Sterically stabilized liposomes: improvements in pharmacokinetics and antitumor therapeutic efficacy. *Proceedings of the National Academy of Sciences* **1991**, *88* (24), 11460-11464.
13. Allen, T. M.; Hansen, C. Pharmacokinetics of stealth versus conventional liposomes: effect of dose. *Biochimica et Biophysica Acta (BBA) - Biomembranes* **1991**, *1068* (2), 133-141.
14. Lee, W.; Il An, G.; Park, H.; Sarkar, S.; Ha, Y. S.; Huynh, P. T.; Bhise, A.; Bhatt, N.; Ahn, H.; Pandya, D. N.; Kim, J. Y.; Kim, S.; Jun, E.; Kim, S. C.; Lee, K. C.; Yoo, J. Imaging Strategy that Achieves Ultrahigh Contrast by Utilizing Differential Esterase Activity in Organs: Application in Early Detection of Pancreatic Cancer. *ACS Nano* **2021**.
15. Llop, J.; Gomez-Vallejo, V.; Gibson, N. Quantitative determination of the biodistribution of nanoparticles: could radiolabeling be the answer? *Nanomedicine (Lond)* **2013**, *8* (7), 1035-8.
16. Harrington, K. J.; Mohammadtaghi, S.; Uster, P. S.; Glass, D.; Peters, A. M.; Vile, R. G.; Stewart, J. S. Effective targeting of solid tumors in patients with locally advanced cancers by radiolabeled pegylated liposomes. *Clin Cancer Res* **2001**, *7* (2), 243-54.
17. Lammers, T.; Rizzo, L. Y.; Storm, G.; Kiessling, F. Personalized Nanomedicine. *Clinical Cancer Research* **2012**, *18* (18), 4889.
18. Golombek, S. K.; May, J.-N.; Theek, B.; Appold, L.; Drude, N.; Kiessling, F.; Lammers, T. Tumor targeting via EPR: Strategies to enhance patient responses. *Advanced drug delivery reviews* **2018**, *130*, 17-38.

19. Kim, Y.; Kwak, H. S.; Kim, C. S.; Chung, G. H.; Han, Y.; Lee, J. Hepatocellular carcinoma in patients with chronic liver disease: Comparison of SPIO-enhanced MR imaging and 16-detector row CT. *Radiology* **2006**, *238*, 531-541.
20. van Dam, G. M.; Themelis, G.; Crane, L. M. A.; Harlaar, N. J.; Pleijhuis, R. G.; Kelder, W.; Sarantopoulos, A.; de Jong, J. S.; Arts, H. J. G.; van der Zee, A. G. J.; Bart, J.; Low, P. S.; Ntziachristos, V. Intraoperative tumor-specific fluorescence imaging in ovarian cancer by folate receptor- $\alpha$  targeting: first in-human results. *Nature Medicine* **2011**, *17* (10), 1315-1319.
21. Alam, I. S.; Steinberg, I.; Vermesh, O.; van den Berg, N. S.; Rosenthal, E. L.; van Dam, G. M.; Ntziachristos, V.; Gambhir, S. S.; Hernot, S.; Rogalla, S. Emerging Intraoperative Imaging Modalities to Improve Surgical Precision. *Mol Imaging Biol* **2018**, *20* (5), 705-715.
22. Voskuil, F. J.; Steinkamp, P. J.; Zhao, T.; van der Vegt, B.; Koller, M.; Doff, J. J.; Jayalakshmi, Y.; Hartung, J. P.; Gao, J.; Sumer, B. D.; Witjes, M. J. H.; van Dam, G. M.; Albaroodi, Y.; Been, L. B.; Dijkstra, F.; van Etten, B.; Feng, Q.; van Ginkel, R. J.; Hall, K.; Havenga, K.; Haveman, J. W.; Hemmer, P. H. J.; Jansen, L.; de Jongh, S. J.; Kats-Ugurlu, G.; Kelder, W.; Kruijff, S.; Kruithof, I.; van Loo, E.; Roodenburg, J. L. N.; Shenoy, N.; Schepman, K. P.; de Visscher, S. A. H. J.; the, S. s. g. Exploiting metabolic acidosis in solid cancers using a tumor-agnostic pH-activatable nanoprobe for fluorescence-guided surgery. *Nature Communications* **2020**, *11* (1), 3257.
23. Sgouros, G.; Bodei, L.; McDevitt, M. R.; Nedrow, J. R. Radiopharmaceutical therapy in cancer: clinical advances and challenges. *Nature Reviews Drug Discovery* **2020**, *19* (9), 589-608.
24. Varghese, J.; Rohren, E.; Guofan, X. Radioiodine Imaging and Treatment in Thyroid Disorders. *Neuroimaging Clinics of North America* **2021**, *31* (3), 337-344.

25. Fani, M.; Nicolas, G. P.; Wild, D. Somatostatin Receptor Antagonists for Imaging and Therapy. *J Nucl Med* **2017**, *58* (Suppl 2), 186783.
26. Prasad, V.; Steffen, I. G.; Pavel, M.; Denecke, T.; Tischer, E.; Apostolopoulou, K.; Pascher, A.; Arsenic, R.; Brenner, W. Somatostatin receptor PET/CT in restaging of typical and atypical lung carcinoids. *EJNMMI Res* **2015**, *5* (1), 015-0130.
27. Rolleman, E.; Melis, M.; Valkema, R.; Boerman, O.; Krenning, E.; de Jong, M. Kidney protection during peptide receptor radionuclide therapy with somatostatin analogues. *European journal of nuclear medicine and molecular imaging* **2009**, *37*, 1018-31.
28. Virgolini, I.; Decristoforo, C.; Haug, A.; Fanti, S.; Uprimny, C. Current status of theranostics in prostate cancer. *Eur J Nucl Med Mol Imaging* **2018**, *45* (3), 471-495.
29. Kratochwil, C.; Flechsig, P.; Lindner, T.; Abderrahim, L.; Altmann, A.; Mier, W.; Adeberg, S.; Rathke, H.; Röhrich, M.; Winter, H.; Plinkert, P. K.; Marme, F.; Lang, M.; Kauczor, H.-U.; Jäger, D.; Debus, J.; Haberkorn, U.; Giesel, F. L. <sup>68</sup>Ga-FAPI PET/CT: Tracer Uptake in 28 Different Kinds of Cancer. *Journal of Nuclear Medicine* **2019**, *60* (6), 801.
30. Dijkers, E.; Oude Munnink, T.; Kosterink, J.; Brouwers, A. H.; Jager, P. L.; Jong, J. R.; Dongen, G. A.; Schröder, C. P.; Hooge, M.; de Vries, E. Biodistribution of <sup>89</sup>Zr-trastuzumab and PET Imaging of HER2-Positive Lesions in Patients With Metastatic Breast Cancer. *Clinical pharmacology and therapeutics* **2010**, *87*, 586-92.
31. Keyaerts, M.; Xavier, C.; Heemskerk, J.; Devoogdt, N.; Everaert, H.; Ackaert, C.; Vanhoeij, M.; Duhoux, F. P.; Gevaert, T.; Simon, P.; Schallier, D.; Fontaine, C.; Vaneycken, I.; Vanhove, C.; De Greve, J.; Lamote, J.; Caveliers, V.; Lahoutte, T. Phase I Study of <sup>68</sup>Ga-HER2-

Nanobody for PET/CT Assessment of HER2 Expression in Breast Carcinoma. *Journal of Nuclear Medicine* **2016**, *57* (1), 27.

32. Rossin, R.; Renart Verkerk, P.; van den Bosch, S. M.; Vulders, R. C. M.; Verel, I.; Lub, J.; Robillard, M. S. In Vivo Chemistry for Pretargeted Tumor Imaging in Live Mice. *Angewandte Chemie International Edition* **2010**, *49* (19), 3375-3378.

33. Stéen, E. J. L.; Jørgensen, J. T.; Johann, K.; Nørregaard, K.; Sohr, B.; Svatunek, D.; Birke, A.; Shalgunov, V.; Edem, P. E.; Rossin, R.; Seidl, C.; Schmid, F.; Robillard, M. S.; Kristensen, J. L.; Mikula, H.; Barz, M.; Kjær, A.; Herth, M. M. Trans-Cyclooctene-Functionalized PeptoBrushes with Improved Reaction Kinetics of the Tetrazine Ligation for Pretargeted Nuclear Imaging. *ACS Nano* **2020**, *14* (1), 568-584.

34. Hofman, M. S.; Violet, J.; Hicks, R. J.; Ferdinandus, J.; Thang, S. P.; Akhurst, T.; Iravani, A.; Kong, G.; Ravi Kumar, A.; Murphy, D. G.; Eu, P.; Jackson, P.; Scalzo, M.; Williams, S. G.; Sandhu, S. [(177)Lu]-PSMA-617 radionuclide treatment in patients with metastatic castration-resistant prostate cancer (LuPSMA trial): a single-centre, single-arm, phase 2 study. *Lancet Oncol* **2018**, *19* (6), 825-833.

35. Rathke, H.; Flechsig, P.; Mier, W.; Bronzel, M.; Mavriopoulou, E.; Hohenfellner, M.; Giesel, F. L.; Haberkorn, U.; Kratochwil, C. Dosimetry Estimate and Initial Clinical Experience with <sup>90</sup>Y-PSMA-617. *Journal of Nuclear Medicine* **2019**, *60* (6), 806.

36. Loktev, A.; Lindner, T.; Burger, E.-M.; Altmann, A.; Giesel, F.; Kratochwil, C.; Debus, J.; Marme, F.; Jaeger, D.; Mier, W.; Haberkorn, U. Development of novel FAP-targeted radiotracers with improved tumor retention. *Journal of Nuclear Medicine* **2019**, jnumed.118.224469.

37. Watabe, T.; Liu, Y.; Kaneda-Nakashima, K.; Shirakami, Y.; Lindner, T.; Ooe, K.; Toyoshima, A.; Nagata, K.; Shimosegawa, E.; Haberkorn, U.; Kratochwil, C.; Shinohara, A.; Giesel, F.; Hatazawa, J. Theranostics Targeting Fibroblast Activation Protein in the Tumor Stroma: (64)Cu- and (225)Ac-Labeled FAPI-04 in Pancreatic Cancer Xenograft Mouse Models. *J Nucl Med* **2020**, *61* (4), 563-569.
38. Baxter, L. T.; Jain, R. K. Transport of fluid and macromolecules in tumors. IV. A microscopic model of the perivascular distribution. *Microvasc Res* **1991**, *41* (2), 252-72.
39. Saga, T.; Neumann, R. D.; Heya, T.; Sato, J.; Kinuya, S.; Le, N.; Paik, C. H.; Weinstein, J. N. Targeting cancer micrometastases with monoclonal antibodies: a binding-site barrier. *Proc Natl Acad Sci U S A* **1995**, *92* (19), 8999-9003.
40. Yang, E. Y.; Shah, K. Nanobodies: Next Generation of Cancer Diagnostics and Therapeutics. *Frontiers in Oncology* **2020**, *10*.
41. Holliger, P.; Hudson, P. J. Engineered antibody fragments and the rise of single domains. *Nature Biotechnology* **2005**, *23* (9), 1126-1136.
42. Verhoeven, M.; Seimbille, Y.; Dalm, S. U. Therapeutic Applications of Pretargeting. *Pharmaceutics* **2019**, *11* (9).